Ca and S takes place approximately in the direction of the *c* axis. The intermediate axis of these ellipsoids lies in the direction of the *b* axis. The directions of the ellipsoids for O(1) and O(11) are similar to those for Ca and S except that the intermediate axis is inclined to the *b* axis (Table 6). For atom O(*W*) the directions of the ellipsoid are different from those of the other atoms and the greatest thermal motion is more nearly in line with the least thermal motion of atoms O(1), O(11), Ca and S. Its intermediate axis is inclined to the *b* axis (Table 6).

The authors wish to thank Professor H. Freeman and staff of the Chemistry Department of the University of Sydney for instructing them in the use of the Supper equi-inclination Weissenberg diffractometer and for supplying them with copies of the crystallographic computer programs used in the work.

References

ATOJI, M. & RUNDLE, R. E. (1958). *J. Chem. Phys.* **29**, 1306–1311.
BRAGG, W. L. (1937). *Atomic Structure of Minerals*, p. 130. New York: Cornell Univ. Press.
BUSING, W. R., MARTIN, K. O. & LEVY, H. A. (1962). *ORFLS*. Report ORNL-TM-305, Oak Ridge National Laboratory, Oak Ridge, Tennessee.
BUSING, W. R., MARTIN, K. O. & LEVY, H. A. (1964). *ORFEE*. Report ORNL-TM-306, Oak Ridge National Laboratory, Oak Ridge, Tennessee.
COLE, W. F. & LANCUCKI, C. J. (1965). *Rev. Sci. Instrum.* **36**, 1669–1670.
COLE, W. F. & LANCUCKI, C. J. (1972*a*). *Nature, Phys. Sci.* **238**, 95–96.
COLE, W. F. & LANCUCKI, C. J. (1972*b*). *Nature, Phys. Sci.* **240**, 48.
COLE, W. F. & LANCUCKI, C. J. (1973). *Nature, Phys. Sci.* **242**, 104–105.
DENNE, W. A. & JONES, D. W. (1969). *Z. Kristallogr.* **130**, 314–317.
FREEMAN, H. C., GUSS, J. M., NOCKOLDS, C. E., PAGE, R. & WEBSTER, A. (1970). *Acta Cryst.* A**26**, 149–152.
HASS, M. & SUTHERLAND, G. B. B. M. (1956). *Proc. Roy. Soc.* A**236**, 427–445.
HUBER-BUSER, E. (1971). *Z. Kristallogr.* **133**, 150–167.
International Tables for X-ray Crystallography (1962). Vol. III, pp. 204–205 and p. 272. Birmingham: Kynoch Press.
MIRKIN, L. I. (1964). *Handbook of X-ray Analysis of Polycrystalline Materials*, pp. 326, 327. New York: Consultants Bureau.
ROUSSET, A. & LOCHET, R. (1945). *J. Phys. Radium*, **6**, 57–61.
SEIDL, V., KNOP, O. & FALK, M. (1969). *Canad. J. Chem.* **47**, 1361–1368.
WEISS, O., COCHRAN, W. & COLE, W. F. (1948). *Acta Cryst.* **1**, 83–88.
WOOSTER, W. A. (1936). *Z. Kristallogr.* **94**, 375–396.

Acta Cryst. (1974). B**30**, 929

Electron Diffraction and the Structure of α-N_2

BY J. A. VENABLES AND C. A. ENGLISH*

School of Mathematical and Physical Sciences, University of Sussex, Brighton, BN1 9QH, England

(*Received* 11 *June* 1973; *accepted* 18 *September* 1973)

Electron diffraction patterns have been obtained from annealed single crystals of α-N_2. The {100} patterns were found to be particularly suitable for resolving the controversy as to whether α-N_2 has the *Pa*3 or $P2_13$ structure. A quantitative comparison of these patterns with calculated intensities was used to set a (conservative) upper limit of 0·05 Å for the displacement of the centre of the N_2 molecule from the *Pa*3 structure. This and other more qualitative evidence strongly suggests that the structure is in fact *Pa*3. Twins on {111} planes were observed and were shown to give rise to some reflexions which are forbidden by *Pa*3 symmetry. The possibility is discussed that twinning could explain a previous X-ray observation of isolated reflexions which were not consistent with the *Pa*3 structure.

1. Introduction

The exact structure of the low temperature α-phase of solid nitrogen has been under discussion since the first X-ray work of Vegard (1929) and Ruhemann (1932). The structure proposed by Ruhemann was *Pa*3 cubic, in which the centres of the N_2 molecules are on a f.c.c. lattice, but each molecule points in a different ⟨111⟩ direction. The Vegard structure is essentially similar but the centre of a molecule is displaced by a small distance, *r*, along the ⟨111⟩ direction parallel to the axis of that molecule. This displacement lowers the symmetry to $P2_13$, which is a non-centrosymmetric structure.

Many diffraction experiments have been performed in an attempt to decide which structure is correct. X-ray powder patterns (Bolz, Boyd, Mauer & Peiser,

* Present address: A.E.R.E., Harwell, Didcot, Berkshire, England.

1959; Schuch & Mills, 1970) and electron diffraction from both powder samples and single crystals (Hörl & Marton, 1962; Venables, 1970) have failed to show the reflexions which indicate departures from *Pa*3 symmetry. However, perhaps the most thorough investigation was an X-ray single-crystal study by Jordan, Smith, Streib & Lipscomb (1964) in which two reflexions, {052} and {051}, forbidden for the *Pa*3 structure, were found at several points in the reciprocal lattice. On this basis, they concluded that the structure was $P2_13$ and that the displacement, r, was about 0·17 Å. A recent refinement of these same data by La Placa & Hamilton (1972) gave $r=0{\cdot}16\pm0{\cdot}02$ Å. In addition, piezoelectric resonance has been observed in α-N_2 by Brookeman & Scott (1972) and this has been taken as proof positive that the structure is not centrosymmertic and therefore $P2_13$. Another qualitative indication of the non-centrosymmetric structure has been given by Watchel (1972), who observed coincidences of infrared absorption peaks with Raman frequencies, although several previous investigations had failed to detect them.

There are however several disturbing features about these results. Firstly, the theories of cohesion of van der Waals crystals are consistent with the *Pa*3 structure for N_2 but not with $P2_13$. As can be seen from the calculations of Goodings & Henkelman (1971), an extra term in the cohesive energy is required to obtain a non-zero value of r; for $r=0{\cdot}16$ Å this term must yield at least 4% of the cohesive energy. This is a large amount to be accounted for, especially as the 4% must be a difference between the displaced and undisplaced positions; the absolute magnitude of this mysterious energy must surely be much larger than this. As pointed out by Bolz *et al.* (1959), it is very unusual to find a centrosymmetric molecule in a non-centrosymmetric space group. If α-N_2 has the $P2_13$ structure, this is the only non-centrosymmetric structure exhibited by the homonuclear diatomic molecular solids (English & Venables, 1973). Secondly, there were clearly some experimental difficulties in obtaining the single crystal X-ray patterns (Jordan *et al.*, 1964). Of over 20 single crystals of β-N_2 cooled through the β–α transition, only one yielded a single crystal of α-N_2, and this was used for the structure determination. Although this crystal gave several examples of {052} and {051} reflexions, there are many more reflexions which should have been detected if the displacement $r\simeq0{\cdot}16$ Å, and if the limit of detectability was as quoted in their Table 3. These reflexions include the 110, 201, 310, 320, 330, 403, 530, 503, 601, 540, 710 and 550. These reflexions appear close to the level of detectability in their paper because Table 3 was calculated for $r=0{\cdot}09$ Å. However for $r\simeq0{\cdot}16$ Å these reflexions should have been well above background since their intensity is proportional to r^2.

In a previous paper by one of us (Venables, 1970) the work of Jordan *et al.* (1964) was unaccountably overlooked. The single-crystal electron-diffraction patterns shown in that paper showed qualitative agreement with the *Pa*3 structure but were not analysed quantitatively. In fact, the difference between the $P2_13$ and *Pa*3 structures is only one of degree; as the displacement r becomes smaller, the *Pa*3 forbidden reflexions become weaker and finally disappear. Thus a diffraction experiment can only establish a maximum possible value of r; if this value is very small, the implication is that the structure is probably *Pa*3. In the present paper further electron-diffraction data from single crystals of α-N_2 are presented. The data are analysed to show that the displacement of the centre of the N_2 molecules from the *Pa*3 structure is, on a most conservative estimate, less than 0·05 Å, and is probably $<0{\cdot}02$ Å. In addition, it is shown that α-N_2 twins very easily on {111} planes and that such twins are invariably produced when thin films are cooled through the β–α transition. These twins give rise to some non-*Pa*3 reflexions, including those reflexions observed by Jordan *et al.* (1964). The possibility that these twins (and other defects) could account for the previous observations favouring the $P2_13$ structure is discussed.

2. Electron-diffraction patterns

2.1. *Experimental procedure and patterns obtained*

Thin films of α-N_2 were condensed from the vapour in an enclosed volume (pressure cell) inside a liquid helium stage in an electron microscope. The procedure was identical to that described by Venables (1970) except that a newer form of pressure cell (English & Venables, 1971) was used. The films were typically condensed at 18°K and annealed in the region 35–40°K for about 5 min before being cooled to 25°K for observation. This procedure produced single crystals which were generally 10 μm across or larger. Use of a selected area aperture to concentrate on areas of the specimen about 3 μm in diameter produced very clear single-crystal cross-grating patterns. These patterns show one plane of the reciprocal lattice and arise because the crystal is bent; the diffraction spots come principally from that part of the crystal in the field of view which is near to the diffracting position.

The difference in diffraction from the *Pa*3 and $P2_13$ structures is principally that, in *Pa*3, reflexions of the type $0kl$, k odd, are forbidden whereas in $P2_13$ they are not. In both structures reflexions $\{00l\}$, l odd, are forbidden and cyclic and anticyclic permutations of $\{hkl\}$ are not equivalent. Thus, although all diffraction patterns can be used to discuss the structure problem, the {100} type patterns are by far the most useful as they would contain all the *Pa*3-forbidden reflexions [$\{0kl\}$, k odd]} if they were present. An example of such a {100} pattern is shown in Fig. 1(*a*), and is indexed in Fig. 1(*b*). This pattern does not show any examples of the *Pa*3-forbidden reflexions, even though there are some 16 places on the pattern where they could be observed if they were present. This is typical of several such patterns taken on different crystals.

As such, this is strong qualitative evidence that the structure is *Pa*3.

In order to establish the maximum value of the displacement, r, using these electron-diffraction patterns we need simple expressions for the intensities of the interesting reflexions, which take into account the bent nature of the crystal and the occurrence of dynamic diffraction effects. Double diffraction occurs very frequently in these foils and gives rise to *Pa*3 forbidden spots. However, in the {100} patterns, in contrast to all others, we are fortunate in that the weak (or non-existent) $\{0kl\}$, k odd, reflexions are not coupled by double diffraction to the strong $\{0kl\}$, k even, reflexions. This makes an estimate of the maximum displacement feasible using these patterns, and this is done in the next section.

2.2. *Estimation of the maximum displacement, r, from {100} patterns*

In order to estimate the maximum value of the displacement, r, of the centre of the N_2 molecules from the *Pa*3 position, it is necessary to measure the intensities of reflexions quantitatively (both observed and unobserved) and to compare these measurements with a suitable theory of electron diffraction from a bent crystal. The operations involved are described below.

More than ten {100} patterns qualitatively similar to Fig. 1(*a*) have been obtained from different α-N_2 crystals. Of these, three have been analysed in detail by taking scans along the $\{0kl\}$, l constant, rows using a Hilger and Watts microdensitometer. These rows contain both the *Pa*3-allowed and non-allowed reflexions. The scans were accurately adjusted to go through the centres of the spots by use of a plate holder with a vernier angular adjustment. The detectability limit for the non-observed reflexions was estimated at three times the background noise on the densitometer trace. This is in fact a conservative estimate, since, when twin spots of this size were observed in these same positions (§ 2.4), they were very readily identifiable because the shape of a diffraction spot is very different from that of the noise. Also no attempt was made to reduce this noise by adjusting the slit geometry, optics or electronics of the densitometer.

A proper theory of electron-diffraction intensities from a bent crystal requires a detailed knowledge of the form and thickness of the crystal observed and a complete dynamical diffraction calculation of all the interacting beams. Such a calculation is pointless for crystals of α-N_2 which bend and evaporate appreciably while the diffraction patterns are being taken. The approximate treatment detailed in the Appendix is quite satisfactory for the present purpose; it leads to the following equation:

$$\xi_w^2 > (g_s/g_w) \,.\, (\pi\xi_s t) \,.\, (I_s/I_w) \,. \qquad (1)$$

In equation (1), ξ_w is the value of the extinction distance of an unobserved (weak) reflexion whose limit of detectability is I_w; ξ_s is the extinction distance for an observed (strong) reflexion whose intensity is measured as I_s; t is the crystal thickness and g_s, g_w, are the lengths of the reciprocal lattice vectors to the reflexions s and w respectively.

In order to estimate the minimum value of ξ_w and hence the maximum value of the displacement r, using equation (1), we need calculated values of the various ξ_g for suitable models of the α-N_2 structure, and estimates of the foil thickness, t. Computations of ξ_g and the corresponding Fourier coefficients of the lattice potential V_g have been made for the *Pa*3 structure and for $P2_13$ structures with $r = 0{\cdot}09$, $0{\cdot}17$ and $0{\cdot}30$ Å. Calculations have been done for a N–N bond length of $1{\cdot}05$ and $1{\cdot}10$ Å: an isotropic temperature factor has been included with a Debye temperature of 68 °K. The calculations were quite standard and some of the *Pa*3 values were reported in the previous paper (Venables, 1970). The difference between the $1{\cdot}05$ and $1{\cdot}10$ Å bond length is marked only for those few high-order ($h^2+k^2+l^2 \simeq 20$–30) reflexions which are calculated to be very weak. The temperature effects are not very marked; the calculations were performed for $T = 20$ °K and the experimental patterns were usually taken at about 25 °K. As expected, the result $V_g \sim \xi_g^{-1} \sim r$ was obtained for *Pa*3 non-allowed reflexions for small values of r. Thus the maximum experimentally allowed value of r can be obtained from each *Pa*3 non-allowed reflexion by comparing the experimental minimum value of ξ_w obtained from equation (1) with the computed result $(r\xi_g) = \text{constant}$.

In order to be sure that the estimate of r is a genuine maximum, it was assumed that everything was acting against the detection of the *Pa*3-forbidden spots. Thus a value of t was assumed which is certainly too small (2000 Å); I_w was generously large ($3\times$ background noise); 'forbidden' spots were only included if they were between two observed 'allowed' spots; and dynamic diffraction effects were made unimportant by choosing to measure the value of ξ_w in equation (1) relative to the allowed reflexion which had the smallest value of $(g_s \,.\, \xi_s \,.\, I_s)$ of all the spots in the pattern. Finally, in converting ξ_w(minimum) to r(maximum), the computation which gave the maximum value of the product $(r\xi_g)$ was used.

The results of the analysis of part of Fig. 1(*a*) are displayed in Fig. 2 in terms of the computed values of the Fourier coefficients of the lattice potential, V_g, and the values measured as described above. The intensities were scaled to the 'weakest' observed reflexion, 021. For the observed reflexions, the estimated values of V_g are within about a factor of three of the calculated values; the differences between theory and experiment shows the extent of double diffraction effects along and between the rows and intensity variations due to crystal thickness effects. For the non-observed reflexions the calculated value of V_g for $r = 0{\cdot}17$ Å is compared with the maximum possible value obtained by the procedure given above. It is seen that if r has this value all ten *Pa*3-forbidden reflexions shown on Fig. 2

should have been observed. Since $I_w \sim V_w^2$ it is also seen that the spots 011 and 012 should have appeared with a signal to noise ratio of at least 150. This means that the intensity of the 012 spot, for example, should be at least one third of 021, which it clearly is not. There is therefore no doubt that the displacement r cannot be as large as the $r = 0{\cdot}16 \pm 0{\cdot}02$ Å determined by La Placa & Hamilton (1972).

The non-observed reflexions set upper limits to r of varying sensitivity. In total, we have obtained from the three plates analysed quantitatively, 5 observations which give $r < 0{\cdot}03$ Å, 14 which give $r < 0{\cdot}05$ Å, and 30 which give $r < 0{\cdot}10$ Å. The most sensitive reflexions are {012}, {011}, {031}, {052}, {033} and {034}. We are therefore quite certain that $r < 0{\cdot}05$ Å, and that this is a conservative estimate. Use of less conservative criteria would set a limit of about 0·02 Å.

2.3. *Other evidence in favour of the Pa3 structure*

On all patterns other than the {100} patterns discussed in the last section, *Pa*3-forbidden reflexions can arise by double diffraction even if the structure *is Pa*3. An example of a {111} pattern is shown in Fig. 3(*a*), where the $\{1\bar{1}0\}$ and $\{3\bar{3}0\}$ spots appear. Analysis of this pattern on the same basis as above gave values of r which are close to the previously proposed $P2_13$ structure. However, it is relatively easy to prove that these spots arise from double diffraction, probably involving the strong $\{2\bar{2}0\}$ and $\{3\bar{2}\bar{1}\}$ reflexions. By increasing the intermediate lens current slightly, a low-magnification picture of the spatial distribution of intensity in each spot is obtained. For each of the 'allowed' reflexions, a bend contour is seen as a line which crosses the field of view. The spots which arise from double diffraction remain as a small weak spot, which originates from the position where the two contours concerned cross. The picture corresponding to Fig. 3(*a*) is shown in Fig. 3(*b*), where the $\{1\bar{1}0\}$ and $\{3\bar{3}0\}$ reflexions do not appear as bend contours, but only as weak dots.

Similar pictures have been taken of these 'expanded diffraction patterns' in many other orientations with the same result; the non-*Pa*3 reflexions arise from double diffraction. This is in fact a very powerful crystallographic technique, as has been shown recently by Steeds, Tatlock & Hampson (1973).

For certain rows of high-order reflexions, the predicted intensities for the *Pa*3 and $P2_13$ (0·17 Å) structures are considerably different, even though 'forbidden' reflexions are not necessarily involved. Under conditions when double diffraction is not strong, the visually estimated intensities in these rows agreed much better with the *Pa*3 structure. All these types of diffraction patterns provide qualitative evidence for the *Pa*3 structure.

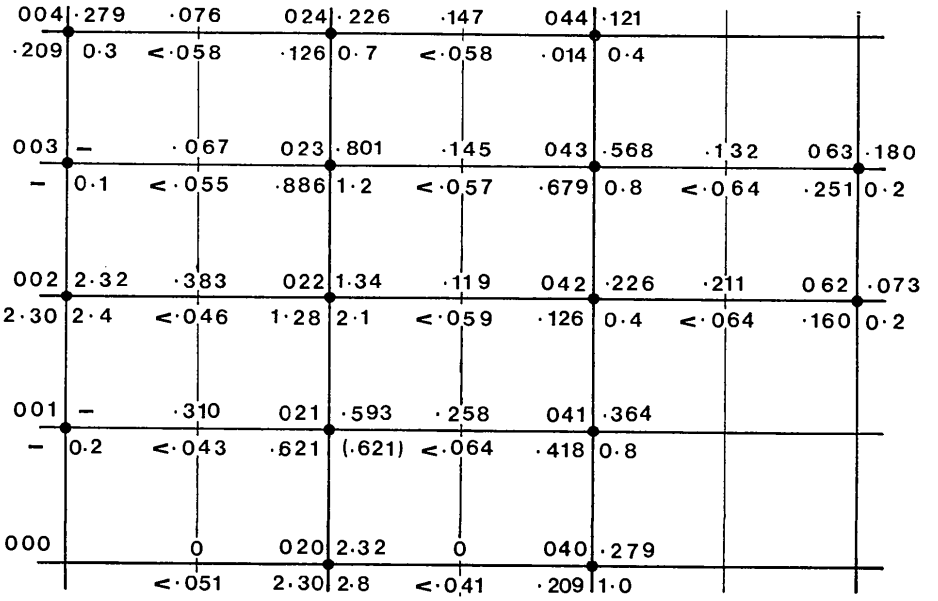

hkl	Vg (P 2₁3)
Vg (Pa 3)	Vg (measured)

Vg (P 2₁3)
Vg (measured)

Fig. 2. Quantitative interpretation of part of Fig. 1(*a*). The values of $V_g(P2_13)$ are calculated for $r = 0{\cdot}17$ Å and a N–N bond length of 1·05 Å; $V_g(Pa3)$ is for a bond length of 1·10 Å. All values are in eV. For the *Pa*3-forbidden reflexions with k odd, the index hkl and $V_g(Pa3)$, which is zero, are both omitted. The indexing is however clear from the position in the diagram.

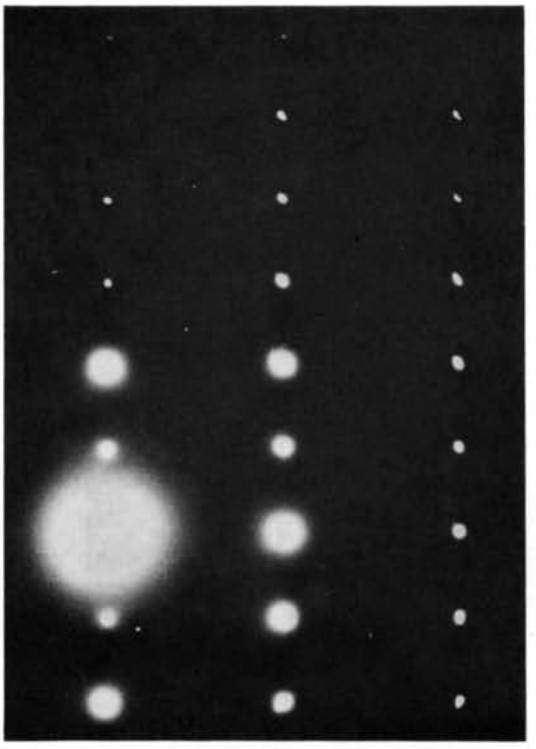

(a)

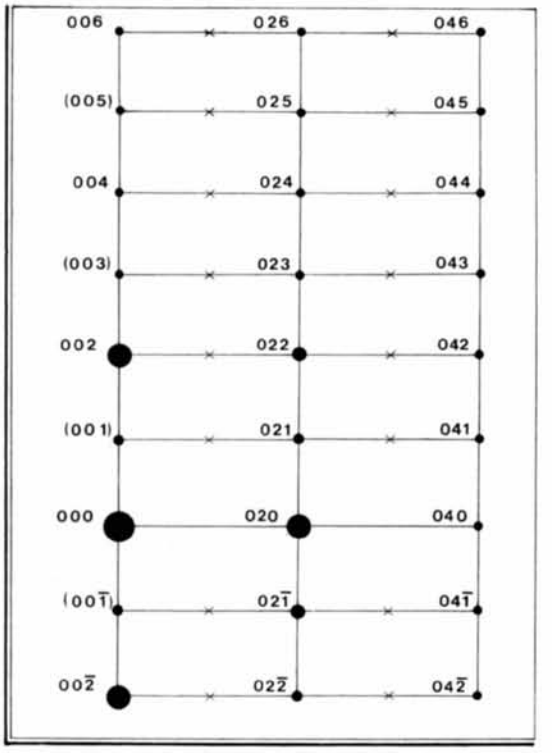

(b)

Fig. 1. (*a*) Electron diffraction pattern of α-N_2 in (100) orientation. (*b*) Indexing of (*a*). The observed reflexions are shown as a dot, the *Pa*3 non-allowed reflexions which are not observed are shown with a cross, and reflexions which arise from double diffraction are indexed in brackets.

[*To face p.* 932

2.4. *Twins in* α-N_2

Annealing twins have been observed very frequently in α-N_2, both in the diffraction patterns and in the corresponding electron micrographs. Examples have been given previously (Venables, 1970). These twins have $\{111\}$ coherent boundaries and $\{11\bar{2}\}$ whose width can be used to measure the foil thickness. Two further facts have been established in the present study. The first is that these twins are invariably produced, not only on annealing the α-phase, but also on cooling through the β–α transition at 35·6°K. The second is that they give rise to some of the *Pa*3-forbidden reflexions. These reflexions are particularly noticeable on the 100 patterns. For example, a (111) twin superimposes a $\{22\bar{1}\}$ pattern on to the $\{100\}$ pattern; this gives rise to extra spots at the following positions: $0\bar{1}4$, 030, $05\bar{2}$, 015, 033, 051. These reflexions have been observed experimentally on several plates.

The reflexions which these twin spots correspond to depends on what type of twins are present. Evidence has been obtained (which will be published separately) which shows that these twins are almost certainly $\{111\}$ reflexion twins, in which the axes are reflected in the $\{111\}$ plane. Since in the α-N_2 structure the $\{hkl\}$ are not equivalent to $\{khl\}$, the reflexion operation (which generates a left-handed set of axes) is not equivalent to the 180° rotation operation associated with a rotation twin. For a reflexion twin the observed extra twin spots arise from the following planes: $0\bar{1}4 \equiv \bar{3}\bar{2}2$, $030 \equiv 1\bar{2}\bar{2}$, $05\bar{2} \equiv 3\bar{2}\bar{4}$, $015 \equiv \bar{3}4\bar{1}$, $033 \equiv \bar{1}4\bar{1}$, $051 \equiv 1\bar{4}\bar{3}$. Reflexion twinning also accounts for the absence of a spot in the 012 position ($012 \equiv \bar{1}20$, which is *Pa*3-forbidden).

In the cases where these extra spots were observed the corresponding micrographs were checked and twins were found. Conversely on the micrograph corresponding to Fig. 1(*a*), which does not show these spots, no twinned regions were seen.

3. Discussion

The obvious question which arises from the present results is whether the previous work which favoured the $P2_13$ structure (Jordan *et al.*, 1964; Brookeman & Scott, 1972; Wachtel, 1972) can be understood in terms of twinning reported in the last section.

The X-ray work (Jordan *et al.*, 1964) has been examined from this point of view. We feel that it is very probable that their crystal contained twins, given the extreme difficulty they had in obtaining the one single crystal. Furthermore, it seems very unlikely that such twins would anneal out, since the α–β transition temperature is so far below the melting point. There are other features which might explain why only $\{052\}$ and $\{051\}$ *Pa*3-forbidden reflexions were observed. The oscillation axis, as described in their paper, is perpendicular to [111] and [100] *i.e.* it is $[0\bar{1}1]$. Assuming that it was impossible to avoid twins running parallel to the axis of the crystal, *i.e.* on $\{111\}$ and $\{\bar{1}11\}$, these two sets of twins would be observed. These two twins would give rise to a maximum of 8 $\{501\}$ spots on the 1st layer lines and 4 $\{5\bar{2}0\}$ spots on the 2nd layer lines, and no new layer lines would be introduced. Also, assuming these to be reflexion twins, the $\{501\}$ and $\{5\bar{2}0\}$ spots are the most intense twin spots in these *Pa*3-forbidden positions, as they are derived from the strong $\{413\}$ and $\{432\}$ reflexions respectively. The $\{501\}$ and $\{5\bar{2}0\}$ are also the only extra spots produced in the $\{h01\}$ and $\{h\bar{2}0\}$ rows within the range of reflexions studied.

A further point is that Jordan *et al.* (1964) showed that the fit was better to $P2_13$ than *Pa*3 even if only *Pa*3-allowed reflexions were used in the structure determination. On examination, this seems to be due primarily to the fact that certain pairs of reflexions are more nearly equal in intensity than they should be according to the *Pa*3 structure. These reflexions are 321, 312; 431, 413; 541, 514; 631, 613; 632, 623. For the first three pairs, twinning on $\{111\}$ can superimpose exactly certain variants of these two different types of reflexions: for example, $3\bar{2}\bar{1} \rightarrow 2\bar{3}1$. For the latter two reflexions this superimposition is not exact, though the twin and matrix reflexions could easily appear on the same oscillation photograph and thus contribute to the same determination of the structure factor, F_{obs}.

The above discussion does not, of course, prove that the previous diffraction data which favoured the $P2_13$ structure were due to twinning, though it does suggest that one should look out for effects of this type in future diffraction experiments. If twinning was in fact responsible for these violations of *Pa*3 symmetry, there should be other weak twin spots present. Several of these would be on the wrong 15° oscillation photograph to be assigned to the corresponding matrix spot. To decide whether this actually was the case, one would have to have access to the original films.

Although the detection of piezo-electricity in α-N_2 (Brookeman & Scott, 1972) is a classic test for the lack of a centre of symmetry, we cannot be convinced that it proves that α-N_2 has the $P2_13$ structure without further discussion. It could be of course that it is $P2_13$ with $r < 0{\cdot}05$ Å, the upper limit established by the present work. Since the piezo-electric resonance experiment was uncalibrated, no indication was obtained of the magnitude of r; it might well be very small, since the method is clearly sensitive and the signals were very weak.

However, it seems to us to be more likely that it was due to unavoidable strains in the crystal and maybe even to the twins which we expect were present, even though the authors took great care taking the crystals through the β–α transformation slowly (Brookeman, McEnnan & Scott, 1971). Recent work by Gannon & Morrison (1973) has shown that N_2 crystals shatter when cooled through the $\beta \rightarrow \alpha$ transition, even when the cooling rate is very slow. In their work it took up to 12 h annealing at just below the transformation temperature for strain-induced birefringence to disappear.

It might even be that the boundaries of $\{111\}$ twins

(*a*)

(*b*)

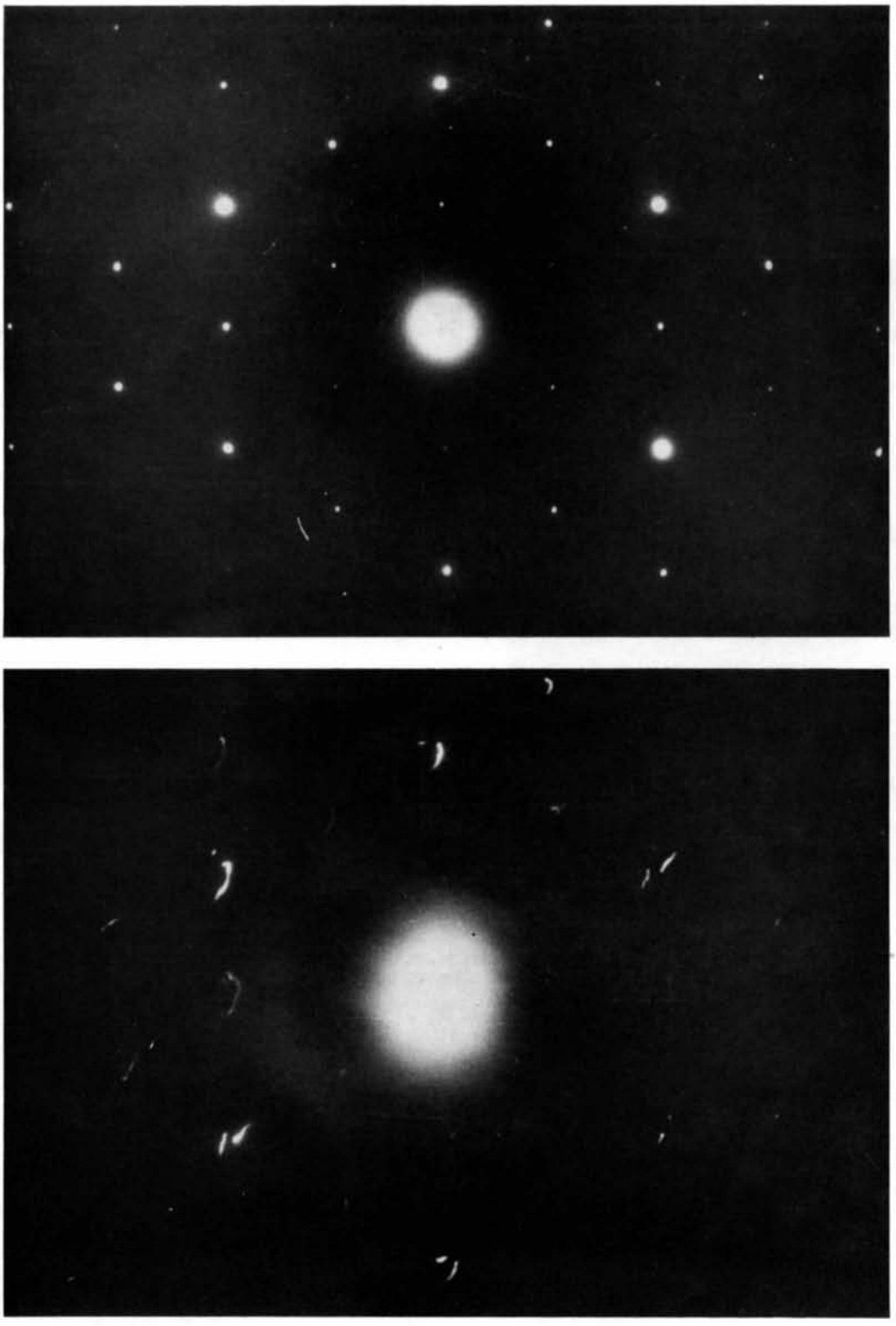

Fig. 3. (*a*) Electron diffraction patter of α-N_2 in (111) orientation. (*b*) 'Expanded diffraction pattern' corresponding to (*a*), showing bend contours for allowed reflexions and weak dots for reflexions $\{1\bar{1}0\}$ and $\{3\bar{3}0\}$, which arise from double diffraction.

could give rise to the piezo-electric effect, because the molecular environment in the boundary cannot be centrosymmetrical.

Essentially similar remarks may be the explanation of the infrared absorption data of Wachtel (1972). Whereas the absorption could be caused by a relatively weak effect spread throughout the crystal, due to the lack of a centre of symmetry implied by the $P2_13$ structure, it could also be due to strains, or to stronger absorption localized near twin and grain boundaries and the cell walls where the departure from centrosymmetry is strong even if the structure itself is $Pa3$. This could explain why several other authors had failed to detect this absorption.

Independent of the above comments, we have shown that the electron diffraction data presented in this paper are inconsistent with a displacement of the centres of the molecules from the centrosymmetric structure by more than (at most) 0·05 Å. Taken with the fact that the theories of cohesion are consistent with $Pa3$ but not with $P2_13$, we are strongly in favour of $Pa3$ as a correct description of α-N_2. However, it would be most desirable to have an independent set of X-ray single-crystal data taken from more than one crystal, whose growth was carefully controlled, and where the possibility of twinning was borne in mind. Until such measurements have been made it is certainly not worth trying to explain theoretically the existence of the $P2_13$ structure.

It is a pleasure to acknowledge a useful letter from Dr R. L. Mills. The help of Mr J. S. Notton for continued maintenance of the electron microscope and for photographic work is gratefully acknowledged. We thank Professors D. A. Goodings, J. A. Morrison and T. A. Scott for useful correspondence. The hospitality of Professors M. Bienfait and R. Kern to one of us (J.A.V.) while this paper was written was appreciated.

APPENDIX

Electron diffraction intensities from a bent crystal

In a bent crystal, the diffraction into a particular reflexion, g, comes from a 'bend contour', which is the locus of points in the crystal where the reciprocal lattice point g is near the reflecting sphere. We assume that the lengths of all bend contours in the field of view are the same, that the crystal presents a range of orientations to the beam within a range θ_R, and that within this range all orientations are equally probable. The range θ_R is large enough to allow the full width of each bend contour to contribute to the diffracted intensity and to account for the presence of all the spots on the cross-grating pattern (typically $\theta_R \simeq 2$–$3°$). Any of these assumptions might be wrong in a particular case by a factor of two (in intensity) either way; but there is no reason to suppose that they introduce systematic errors into the results from arbitrarily chosen crystals.

With these assumptions, the intensity diffracted from a crystal of thickness t into g is given by the standard form (Hirsch, Howie, Nicholson, Pashley & Whelan, 1965)

$$I_g \alpha (2/\theta_R) \int_0^\infty \mathrm{d}\theta (\pi t/\xi_g)^2 \sin^2(\pi t\bar{s})/(\pi t\bar{s})^2 \qquad \text{(A1)}$$

where ξ_g is the extinction distance, $\bar{s} = |(s^2 + \xi_g^{-2})$, s is the deviation from the exact reflecting position, and the element of angle $\mathrm{d}\theta$ is related to s by $\mathrm{d}\theta = \mathrm{d}s/g$. The value of I_g given by equation (A1) depends on whether the scattering is weak (kinematic) or strong (dynamic). For small values of t and/or large values of ξ_g the kinematic limit of (A1) gives the intensity, I_w, of weak reflexions

$$I_w \simeq 2\pi t/(\theta_R \,.\, g_w \,.\, \xi_w^2) \qquad \text{(A2)}$$

since $\int_0^\infty \mathrm{d}x \sin^2 x/x^2 \simeq 1$, where $x = \pi t s$. Equation (A2) arises because diffraction of approximate strength $(\pi t/\xi_w)^2$ occurs over a range of values of s, $|s| \lesssim t^{-1}$, in the thin crystal limit.

For strong reflexions, the intensity, I_s, predicted by equation (A1) varies between zero and a maximum value depending on the thickness, t. This maximum value therefore overestimates the diffracted intensity for an arbitrary thickness, or for a foil containing a range of thicknesses.

The result is

$$I_s \lesssim 2/(\theta_R \,.\, g_s \quad \xi_s)\,; \qquad \text{(A3)}$$

it arises because $|s| \lesssim \xi_g^{-1}$ for strong diffraction to occur.

The above description should be roughly adequate to describe the relative intensities of the $Pa3$ allowed reflexions, using equation (A3), when strong double diffraction effects are absent, and when ξ_s is sufficiently small. It is also quite sufficient to estimate the minimum value of ξ_w for non-observed reflexions using equations (A2) and (A3). In this case I_w is the detectability limit, and we have

$$\xi_w^2 > (g_s/g_w) \,.\, (\pi \xi_s t) \,.\, (I_s/I_w)\,. \qquad (1)$$

In the above treatment we have ignored anomalous absorption effects as they are relatively weak in α-N_2 (Venables, 1970). Ordinary absorption would affect all reflexions equally and so does not affect relative values in equations (A2) (A3) and (1).

Crystal thicknesses have been measured from electron micrographs containing {111} twins (Venables, 1970 and § 2.4) to be in the range 2000–4000 Å. For these thicknesses almost all the $Pa3$-allowed reflexions are diffracting dynamically, whereas, for small r, the $Pa3$ non-allowed reflexions would behave kinematically if they were present. This justifies the use of equation (1) to determine ξ_w(minimum) and r(maximum).

References

BOLZ, L. H., BOYD, M. E., MAUER, F. A. & PEISER, H. S. (1959). *Acta Cryst.* **12**, 247–248.

BROOKEMAN, J. R., MCENNAN, M. M. & SCOTT, T. A. (1971). *Phys. Rev.* B**4**, 3661–3676.

BROOKEMAN, J. R. & SCOTT, T. A. (1972). *Acta Cryst.* B**28**, 983–984.

ENGLISH, C. A. & VENABLES, J. A. (1971). *Proceedings of the 25th Anniversary Meeting of the Electron Microscopy and Analysis Group*, pp. 48–49. To be published (1973). London: Institute of Physics.

GANNON, D. J. & MORRISON, J. A. (1973). *Canad. J. Phys.* **51**, 1590–1592.

GOODINGS, D. A. & HENKELMAN, M. (1971). *Canad. J. Phys.* **49**, 2902–2910.

HIRSCH, P. B., HOWIE, A., NICHOLSON, R. B., PASHLEY, D. W. & WHELAN, M. J. (1965). *Electron Microscopy of Thin Crystals*, pp. 201–202. London: Butterworths.

HÖRL, E. M. & MARTON, L. (1961). *Acta Cryst.* **14**, 11–19.

JORDAN, T. H., SMITH, H. W., STREIB, W. E. & LIPSCOMB, W. N. (1964). *J. Chem. Phys.* **41**, 756–759.

LA PLACA, S. J. & HAMILTON, W. C. (1972). *Acta Cryst.* B**28**, 984–985.

RUHEMANN, M. (1932). *Z. Phys.* **76**, 368–375.

SCHUCH, A. F. & MILLS, R. L. (1970). *J. Chem. Phys.* **52**, 6000–6008.

STEEDS, J. W., TATLOCK, G. J. & HAMPSON, J. (1973). *Nature, Lond.* **241**, 435–439.

VEGARD, L. (1929). *Z. Phys.* **58**, 497–501.

VENABLES, J. A. (1970). *Phil. Mag.* **21**, 147–166.

WATCHEL, E. J. (1972). *J. Chem. Phys.* **57**, 5620–5621.

Acta Cryst. (1974). B**30**, 935

Crystal Structures of Pentacoordinate Phosphorus Compounds. II.* 2-Fluoro-2,2′-spirobis-(1,3,2-benzodioxaphosphole), $(C_6H_4O_2)_2PF$

BY HARTMUT WUNDERLICH† AND DIETRICH MOOTZ†

Max-Planck-Institut für Festkörperforschung, 7 Stuttgart 1, Postfach 1099, Germany (BRD)

(*Received* 19 *November* 1973; *accepted* 21 *November* 1973)

The title compound is orthorhombic, space group $P2_12_12_1$, with $a=11{\cdot}338$ (5), $b=14{\cdot}725$ (5), $c=6{\cdot}750$ (3) Å; $Z=4$. The intensities were measured on an automatic off-line four-circle diffractometer. The structure was solved by Patterson and Fourier techniques and refined by full-matrix least-squares calculations to $R=0{\cdot}04$. The geometry of the pentacoordinate phosphorus atom is considerably distorted from the idealized trigonal bipyramid and may be regarded as intermediate between this and a square pyramid. The axial angle O–P–O is 168·2°, the equatorial angles are 107·3, 106·6, and 146·1°. The P–O bond lengths are 1·659 and 1·658 Å (axial) and 1·628 and 1·625 Å (equatorial). Each catechol residue is connected to one axial and one equatorial oxygen atom, thus leaving an equatorial position for the fluorine atom.

The stereochemistry of pentacoordinate phosphorus is usually associated with the geometry of a trigonal bipyramid [see for example Ugi & Ramirez (1972)]. This model has been established for free molecules with five equal and independent ligands at the phosphorus atom, *e.g.* PF_5 (Hansen & Bartell, 1965). Packing forces, unequal ligands and steric interaction of some of the ligands as a consequence of chelation can be expected to cause deviations from the idealized D_{3h} ($\bar{6}m2$) symmetry. Such deviations have, in fact, often been observed since the first accurate crystal structure determinations of more complex compounds such as pentaphenylphosphorus (Wheatley, 1964), the *N*-methyltrichlorophosphinimine dimer (Hess & Forst, 1966) and a cyclic oxyphosphorane (Spratley, Hamilton & Ladell, 1967).

The title compound is also a cyclic oxyphosphorane, with two bidentate catechol residues and a fluorine atom at the phosphorus atom. Considerations of angular strain and ^{19}F n.m.r. data are consistent with the fluorine atom in the equatorial plane of a trigonal bipyramid and each catechol residue bridging one equatorial and one axial position (Doak & Schmutzler, 1970, 1971). However the fluorine atom, as the ligand with the highest electronegativity, should tend to an axial position (Ugi & Ramirez, 1972); thus the applicability of the trigonal bipyramid model to this molecule seems questionable and the alternative of a square pyramid geometry (Hoffmann, Howell & Muetterties, 1972) may be considered. The structure determination was undertaken in order to settle this point. In the structure presented in the following paper (Wunderlich, 1974) the fluorine atom is replaced by a methyl group. Preliminary accounts of both investigations have appeared elsewhere (Wunderlich & Mootz, 1973; Wunderlich, Mootz, Schmuztler & Wieber, 1973).

* Part I: Wunderlich, Mootz, Schmutzler & Wieber (1974).

† Present address: Lehrstuhl für Strukturchemie und anorganische Chemie, Universität Düsseldorf, 4 Düsseldorf, Germany.